Composite Structures 176 (2017) 547–555

Contents lists available at ScienceDirect

Composite Structures

journal homepage: www.elsevier.com/locate/compstruct

Bond interface design for single lap joints using polymeric additive manufacturing

R. Garcia [a], P. Prabhakar [b,*]

[a] Department of Mechanical Engineering, University of Texas at El Paso, El Paso, TX 79968, USA
[b] Department of Civil & Env. Engineering, University of Wisconsin-Madison, Madison, WI 53706, USA

ARTICLE INFO

Article history:
Received 6 December 2016
Revised 18 March 2017
Accepted 23 May 2017
Available online 31 May 2017

Keywords:
Single lap joints
Adhesively bonded joints
Apparent shear strength
Polymer additive manufacturing
Finite element stress analysis

ABSTRACT

In this paper, the use of polymer additive manufacturing technology, also called 3D printing, for imparting texture to bond regions in adhesively bonded joints is explored. An improvement in the apparent shear strength values of adhesively bonded single lap joints is achieved by fusing structural reinforcements to the adherents through fused deposition modeling (FDM) additive technique. Towards that, computational models were first developed to simulate stress distribution along the overlap region of single lap shear joints, and four models that performed the best were chosen for physical testing. Pure adhesive (PA) joints were manufactured first, followed by the fabrication of 3D-printed adhesive (3D-PA) joints. Peak loads, shear stresses, and failure types were compared between these models. PA joints failed mainly adhesively, resulting in low peak loads and shear strength, whereas, 3D-PA joints registered higher average peak loads and shear strengths (increased by up to ≈832 %) with predominantly cohesive failure. 3D printed reinforcements appear to have imparted higher shear resistance against failure at the bond regions. Overall, using a combined computational and experimental approach, it is established that the 3D printed reinforcements have the potential to drastically improve the apparent shear strength of adhesively bonded single lap joints.

1. Introduction

Automotive and aerospace industries, amongst many others, are exploring routes to improve the quality of joints in an assembled component. Joints are critical regions in structures due to the stress concentrations manifested compared to the members of a component. With increasing applications of fiber reinforced polymer matrix composites (FRPCs) in aircrafts, navy structures and automobiles, novel joining technology to assist the fabrication of large components has become a priority for structural engineers. Conventional materials such as steel or aluminum are joined using fasteners and/or bolted joints, which are not favorable for FRPCs as drilling or cutting may damage fibers causing an adverse effect on their structural integrity. Thus, adhesively bonded joints are becoming a viable option for joining FRPCs.

Advantages of bonded joints over traditional mechanical fasteners are lower structural weight and improved damage tolerance. Despite these advantages, bonded joints in primary load-bearing applications often result in overdesign due to the inclusion of mechanical fasteners for additional safety. This is due to the lack of confidence in adhesively bonded joints for composite joining technology. Mechanics based designs for bonded joints are necessary to facilitate efficient use of composites for lightweight applications. This paper presents the use of additive manufacturing to improve the mechanical behavior of bonded joints by enhancing the load bearing capacity of the bond area.

Aerospace industry was the first to conduct work on adhesively bonded joints in the 1970–80s. An extensive review on the joint strength of adhesive joints for fiber reinforced composites was provided by Matthews et al. [1]. The bond strength for FRPCs depends on various parameters, like, joint configuration, adhesive properties, surface preparation, test methods, environmental conditions, etc. Of these, surface preparation is perhaps one of the most critical in governing the quality of the joint [2]. According to Davis and Bond [3], surface treatment with favorable surface chemistry prior to bonding can result in significant increase in the bond strength resulting in improved durability of adhesive bonds. In order to ensure maximum bond strength, abrasion/solvent cleaning techniques are commonly employed as surface treatment for thermoset composites, like carbon/epoxy or glass/epoxy composites. Other viable options for surface treatments are, grit blasting, acid

* Corresponding author at: 2210 Engineering Hall, 1415 Engineering Drive, Madison, WI 53706, USA.
E-mail address: pprabhakar4@wisc.edu (P. Prabhakar).

http://dx.doi.org/10.1016/j.compstruct.2017.05.060
0263-8223/

etching, laser treatment, etc. A novel method is proposed here that utilizes additive manufacturing to impart engineered structure to adherent surfaces in order to drastically increase the bond strength. It is hypothesized that mechanics dictated gradation of interface modification will further assist in improving the strength and toughness of the adhesive bond.

Adhesively bonded joints can have different geometries depending on the type of application. Commonly studied joints by previous researchers [4] are single-lap, double-lap, scarf, stepped, T-shaped, tubular lap, L-shaped joints, etc. A detailed procedure for the design of adhesively bonded joints, like single, double and step, for composites under static and cyclic loads is given in Chamis and Murthy [5]. Stress distribution within a joint dictates the strength of an adhesively bonded joint, which in turn depends on the geometry of the joint and material properties of adhesive and adherent. Therefore, a detailed analysis of a joint configuration with the corresponding materials is required to evaluate the stress distribution. The joint design should be catered towards minimizing the stress concentrations that catalyze debonding type failure at the composite joint. Especially, peel and cleavage stresses should be suppressed, while maintaining an almost uniform stress distribution along the joint. The effects of stress concentrations are accentuated due to layered nature of fiber reinforced composites. The weak interfaces within the adherents can result in their failure along with joint failure. Therefore, it is essential to improve the mechanical properties of bonded joint regions of a layered composite.

Single-lap joint is one of the most commonly used joint geometry due its simplicity and easiness to fabricate [6]. However, stress concentrations are manifested at the ends of the bond overlap that potentially cause peel damage resulting in their premature failure [7–9]. Previous researchers have explored modifying the adherent geometries [10–12], like tapering, stepping and wavy lap, as possible options to minimize these stress concentrations to improve their load bearing capacity. However, a changing adherent shape is a constraint on the component geometry and may not be favorable for fabrication purposes. Hence, there is a critical need to improve the bond strength while maintaining standard geometries of the adherent. Further, complex joint designs, like T-joint or Pi-joint, that are used to join composites require extensive investigation on the stress distribution and its influence on the overall structural integrity of the component.

Interface design is very critical for bonded joints in FRPCs and a smart designing technique should be developed to minimize the damage and failure incurred by weak bond interfaces. It is hypothesized that improvement in strength and toughness can be achieved by imparting structural texture at the adhesively bonded joint interfaces. Hence, novel technology using additive manufacturing at the bond interfaces has been explored in this paper. The research reported in this paper was split into the following main steps: (1) Conduct single lap shear (SLS) tests on pure epoxy adhesively bonded joints to establish a baseline for apparent shear strength; (2) Analyze the bonded joint systems computationally to determine the stress distributions; (3) Modify the bond design computationally to understand their influence on the distribution of stresses; (4) Enable the optimum designs at the bond regions accurately using fused deposition modeling within polymer additive manufacturing; (5) Conduct single lap shear (SLS) tests on the modified joints to check the influence of the new bond interface designs on the apparent shear strength.

The outline of the paper is as follows: The manufacturing process for pure adhesively bonded joints and modified joints is explained first, followed by the computational modeling of altered bond designs. The experimental approach for testing the single lap joints is described next followed by results, discussion and conclusions.

2. Manufacturing

Single lap shear adhesively bonded joints were examined in this paper following the ASTM D5868-01 standard [13]. The manufacturing process of the bonded joints can be divided into two parts: (1) development of bonded joints using pure adhesive only, and (2) development of the bonded joints incorporating 3D printed designs on the adherents. The joint preparation process for both cases will be discussed next.

2.1. Pure adhesive joints

Two carbon fiber woven epoxy laminate adherents were bonded together using LOCTITE Hysol E-120HP epoxy (refer to Table 1), which was cured at room temperature for 24 h. The adherent substrates used were water-jet cut from a DragonPlate solid woven carbon fiber laminate (2.38 mm thick Matte 30.48 cm × 60.96 cm). A total of 5 joints with dimensions shown in Fig. 1(a) were fabricated and tested.

Bond line thickness of 0.76 ± 0.05 mm was achieved using glass microspheres, which provided a bond line control of 700–800 μm (refer to Table 2 for the measured specimen thicknesses). Due to insufficient information in literature about adhesive to microsphere ratio [15,16,13], the authors decided to use a weight ratio of 10:1 as suggested by the manufacturer. In addition, a 15:1 configuration was used for pure adhesive bond testing in order to examine the influence of microspheres on the strength of the adhesive bond. The microspheres were mixed thoroughly with the resin prior to applying on an overlap area of 6.45 cm^2 of the substrates. C-clamps were used to apply pressure on the overlap area as shown in Fig. 1(b), where equal number of threads above the c-clamp overhead was maintained to ensure comparable values of pressure applied between different joints fabricated. Another approach for manufacturing single lap joints suggested by Boutar et al. [14] was followed, which does not use microspheres. A schematic of the setup is shown in Fig. 1(c), where the bond line thickness was achieved using an aluminum support to raise one of the adherents by the required height. A weight was added onto the same adherent to aid in curing of the adhesive as shown in Fig. 1(d).

2.2. 3D-printed adhesive joints

Manufacturing 3D-printed adhesive (3D-PA) joints using fused deposition modeling (FDM) required printing the interface designs onto the carbon fiber adherents (or substrates) prior to fabricating the joints using epoxy. FORTUS 900mc Stratasys machine was the printer used. The material used to create the interface designs was ABS-M30, which will be referred to as "model" material in this paper. ABS-M30 is up to 25–70% stronger than standard Stratasys ABS material, possessing greater tensile, impact, and flexural

Table 1
Epoxy product characteristics.

Technology	Property
Chemical Type (Resin)	Epoxy
Chemical Type (Hardener)	Polyamide
Appearance (Resin)	Off-white to beige liquid
Appearance (Hardener)	Amber liquid
Appearance (Mixed)	Amber-Beige
Components	Two component – requires mixing
Viscosity	High
Mix Ratio (volume) – Resin:Hardener	2:1
Mix Ratio (weight) – Resin:Hardener	100:46
Cure	Room temperature cure after mixing
Application	Bonding

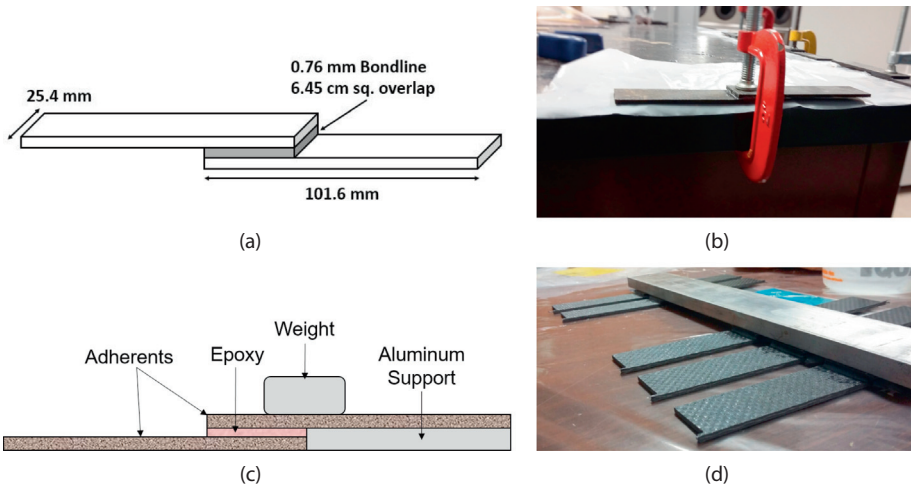

Fig. 1. (a) Dimensions for single lap joint as per the ASTM standard; (b) C-clamps used for applying constant pressure on samples with microspheres; (c) Schematic for pure adhesive joints without microspheres [14]; (d) Physical setup for PA joints without microspheres.

Table 2
Measured specimen thicknesses.

Sample No.	PA (10:1) (mm)	PA (15:1) (mm)	PA (N/B) (mm)	Model 1 (mm)	Model 2 (mm)	Model 3 (mm)	Model 4 (mm)
1	5.50	5.57	5.43	5.54	5.53	5.51	5.51
2	5.57	5.50	5.44	5.50	5.52	5.52	5.49
3	5.48	5.55	5.48	5.57	5.47	5.49	5.48
4	5.50	5.52	5.44	5.53	5.48	5.53	5.49
5	5.56	5.54	5.51	5.51	–	–	–

strength. The model material was extruded at a temperature of 315 °C and the chamber temperature was 95 °C. Note that these temperatures vary for different model materials, such as polycarbonate (PC) or ULTEM 9085. The substrates (or adherents) were exposed to the chamber temperature required by the model material for fifteen minutes prior to printing the model material to check for any damage imparted due to the chamber temperature. The substrates showed no degradation in the material property and the printing process was initiated next.

A new methodology was developed and followed for printing over the nominal thickness of the substrates due to the lack of a standard manufacturing procedure for 3D printing over carbon-fiber substrates. 3D printing machines are generally calibrated in the x, y, and z directions for printing over their corresponding platforms, but, lack the same for composite substrates.

Few challenges encountered during the printing process on substrates are discussed next. The first challenge was to develop a technique for restricting the substrate's free body motion inside the machine chamber caused by the friction between the extruder and the adherent. This was addressed by crafting a fence of 2.54 mm in height tightly around the substrate within a tolerance of ±0.0254 mm, which was designed via computational aided design (CAD) modeling as shown in Fig. 2(a). The area within this fence was assumed to be occupied by the carbon-fiber substrate, and therefore the fence was the same height as that of the substrate.

Upon imposing the boundary conditions on the adherent using the fence fabricated, the next challenge to tackle was to establish a procedure to fuse the ABS-M30 material over the carbon-fiber substrate. The same CAD model used for crafting the fence was utilized for printing the designs on the substrate due to the prior knowledge of their nominal thickness. The desired interface reinforcement pattern was placed only on the joint overlap area of the substrate within the assumed occupied space inside the fence. A tolerance of ±0.254 mm was considered while adding the interface reinforcement on the joint overlap area.

Upon adding the pattern of reinforcements to the CAD model, the file was exported to.stl format for pre-processing in the Stratasys Insight software. This software serves as the medium between the end-user and 3D-printer for creating a building job queue. The parameters altered using Insight were the modeler type (FORTUS 900mc), slice height (0.1778 mm), interior part style (solid-normal), visible surfaces (normal rasters), support style (sparse), model and support tip (T12 tip), model material (ABS-M30), model material color (black), and support material (SR30 support). After applying the preferred settings and running the required slice, support, and toolpath operations, the final step of pre-processing was to insert a pause operator before the first layer of the interface reinforcement. Note that since the slice height used was 0.1778 mm and the design height of the interface reinforcement was 0.76 mm, there were a total of four layers of ABS-M30 material constituting the reinforcement. Hence, the pause was inserted before printing the bottom first layer of the four constituent layers. Typically for this particular 4 layer design, the building job would pause at 88% (i.e. when the surrounding fence was 100% built), allowing the end-user to open the FORTUS 900mc printer door, lower the platform, and safely place the substrate inside the space confined by the fence. Once the adherent was fully secured inside the fence, the printer door was closed and the building job was resumed by the user. The remaining 12% of the building job corresponded to the interface reinforcements, which began to fuse over the carbon-fiber composite substrate inside the printer. The average printing time for a complete 3D-PA substrate reinforcement was approximately 10 min. After the building job reached 100%, the substrate was removed from the 3D printer and optically examined for bond adherence between the ABS-M30 and the carbon-fiber substrate. Also, the interface reinforcements were measured with a caliper for reassuring a 0.76 ± 0.05 mm height

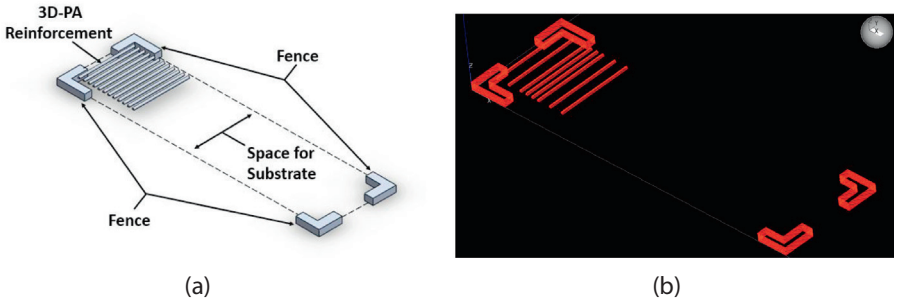

Fig. 2. (a) Schematic diagram of CAD; (b) Stratasys Insight pre-processing of CAD.

(refer to Table 2 for the measured specimen thicknesses), which would provide the bondline control thickness required by the ASTM standard. If either of the above requirements was unsatisfactory, the FORTUS 900mc printer was calibrated in the *z* direction as prescribed by the end-user, and the printing process for the substrate repeated.

Fig. 3 shows the side view of the printed specimens. The horizontal spacing between the design lines were adjusted such that there is enough space for a resin layer between them to assist perfect bonding in the lap joint. Overall, the 3D printing process involved the steps shown in Fig. 4.

Upon printing the interface reinforcement designs on the substrates, the single lap joints were fabricated using a procedure similar to that of the pure adhesive joints. The only difference was that microspheres were not used here as the printed designs provided the required bondline control thickness.

3. Computational approach

A computational model of the adhesively bonded joint specimen was developed (see Fig. 5)) to determine the stress distribution in the bond regions.

Commercially available finite element method software "ABAQUS" was used to model the system. A homogenized model for the carbon-fiber composite adherents was used with adhesive layer at the bonded joint. Effective mechanical properties of the carbon fiber laminate adherents [17], adhesive [18] and the model material [19] (3D printed) are shown in Table 3. The adhesive and ABS-30 M reinforcements were modeled assuming isotropic behavior, which yields $E_{11} = E_{22} = E_{33}$ and $\nu_{12} = \nu_{13} = \nu_{23}$.

The first model generated was the bonded joint specimen with pure epoxy. A displacement of 1.016 mm in tension was applied at both the ends of the specimen along the *x* direction. Maximum principal stress was determined along the centerline of the bonded region and plotted as shown in Fig. 6.

This was followed by modeling the bond region with four different designs as shown in Fig. 7. In the pure epoxy model, the bonded regions experienced significant stresses towards the edges of the bond overlap, as also noted by Banea and Lang [6,20]. Due to these significant stresses, the material is more likely to initiate failure in these regions. The prime objective of the designs imparted to the bonded interface is to improve the bond strength by redistributing the stresses to effectively reduce the risk of failure.

In order to analyze the behavior of the bond interface, partitions were created on the adherents and the bond area due to their complex designs. The region near the bond interface was meshed with fine elements to closely capture the stress distribution, while the rest of the model was coarsely meshed (5.1 mm seed size). A mesh sensitivity study was conducted by refining the local seed size using in the range of 0.0762 mm, 0.0635 mm, and 0.0508 mm. For each seed size, the load–displacement response was determined and no significant change in stress distribution among the

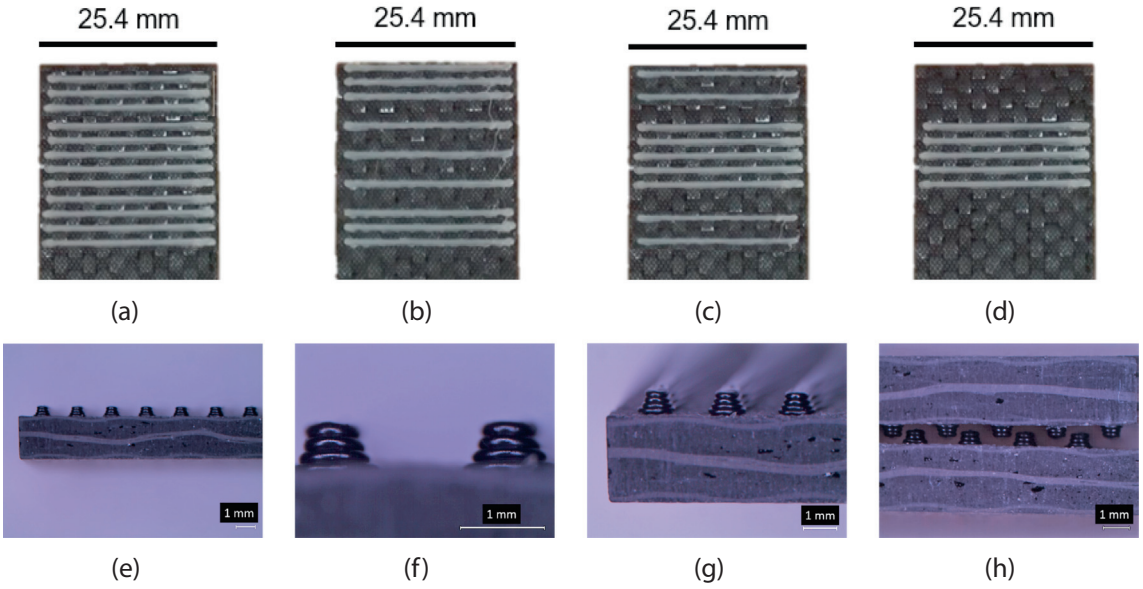

Fig. 3. (a)-(d): Images of the substrate surface with printed reinforcements for Model 1, 2, 3, and 4, respectively; (e)-(h) Digital microscopy of 3D printed substrates with visible gaps in side view of lap joint.

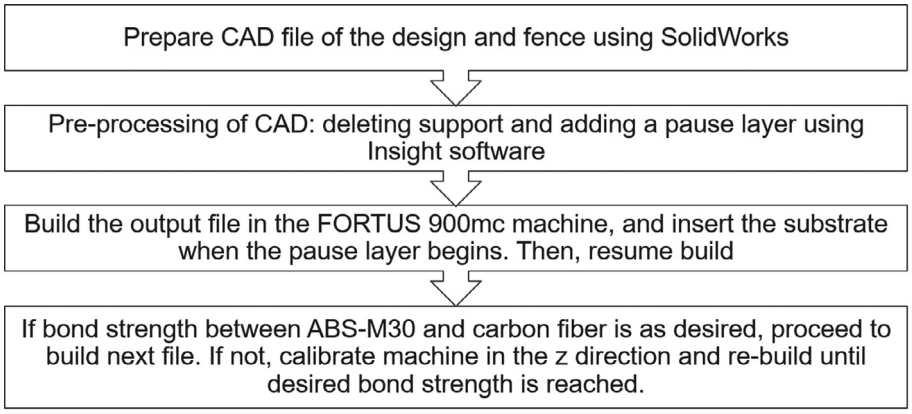

Fig. 4. Flowchart of fused deposition modeling process.

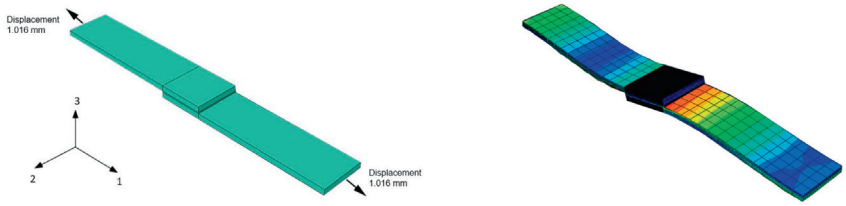

Fig. 5. (a) Undeformed finite element model; (b) Deformed finite element model.

Table 3
List of materials and their assumed mechanical properties.

Material	E_{11} (GPa)	E_{22} (GPa)	E_{33} (GPa)	ν_{12}	ν_{13}	ν_{23}	G_{12} (MPa)	G_{13} (MPa)	G_{23} (MPa)
Adherents	48.02	48.02	1.94	0.2	0.48	0.27	940	770	770
Adhesive	10.34	–	–	0.3	–	–	–	–	–
ABS-30M	2.75	–	–	0.3	–	–	–	–	–

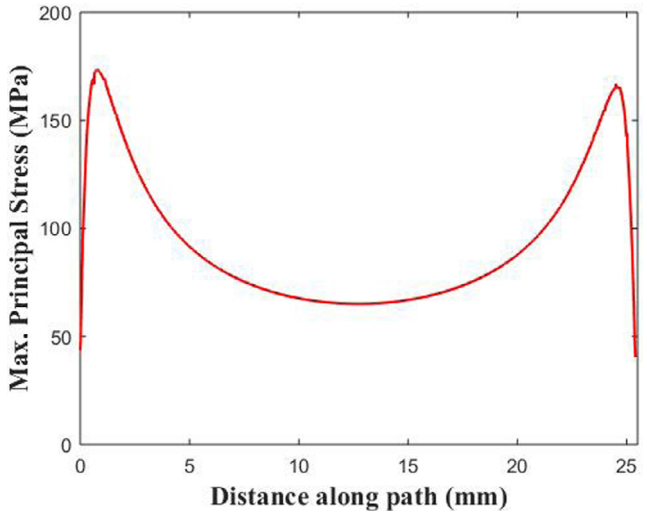

Fig. 6. Maximum principal stress along bonded region center path.

three iterations was observed. The maximum principal, normal and shear stress distribution for all the models are shown in Fig. 8. The distinction in stresses are not very evident from the individual stress distributions (σ_{33} and σ_{13}) shown in Fig. 8 (b) and (c). Hence, maximum principal stresses are compared between different models (Fig. 8 (a)), as they represent the effective response of the bond regions that were modeled assuming isotropic material behavior.

The pure epoxy model displays drastic spikes in the stress values towards the edges of the bond joint, but remains constant in the middle region of the bond overlap area. Among the 3D-PA joint models developed, Model 2 and Model 4 appear to reduce the spike in stress values towards the edges, hence redistributing the stresses in the bond region. This is favorable since reducing the drastic change of stress undergone is more likely to reduce failure. It is notable that for all designs, unlike the uniform behavior observed in the pure epoxy model in the middle, there is a fluctuation in stress/strain at the places were the reinforcements are located. Also, the strain is higher overall for all designs, even the ones that reduced stress. However, stress is more critical to failure than strain, and the models generated an overall uniform distribution that resulted in lower stress changes. Models with uniform stress distribution compared to the pure epoxy case were chosen and printed using polymer additive manufacturing technique.

4. Experimental approach

Single lap shear tests were conducted to determine the apparent shear strength of the single lap joint bonded specimens. Pure epoxy adhesive and 3D-PA joints were tested in the same manner. Single lap shear (SLS) tests were performed on an INSTRON 5969 machine, assuring safety conditions and following protocol regulations [21] and specifications mentioned in ASTM D5868-014 [13].

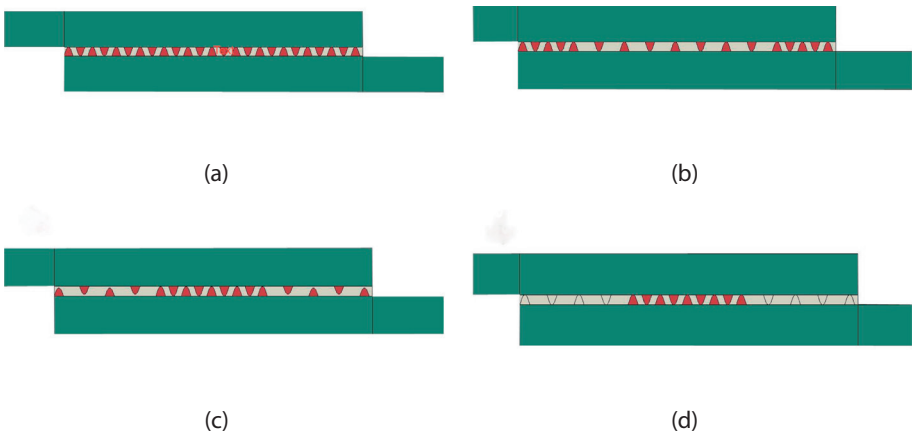

Fig. 7. (a) Model 1; (b) Model 2; (c) Model 3; (d) Model 4.

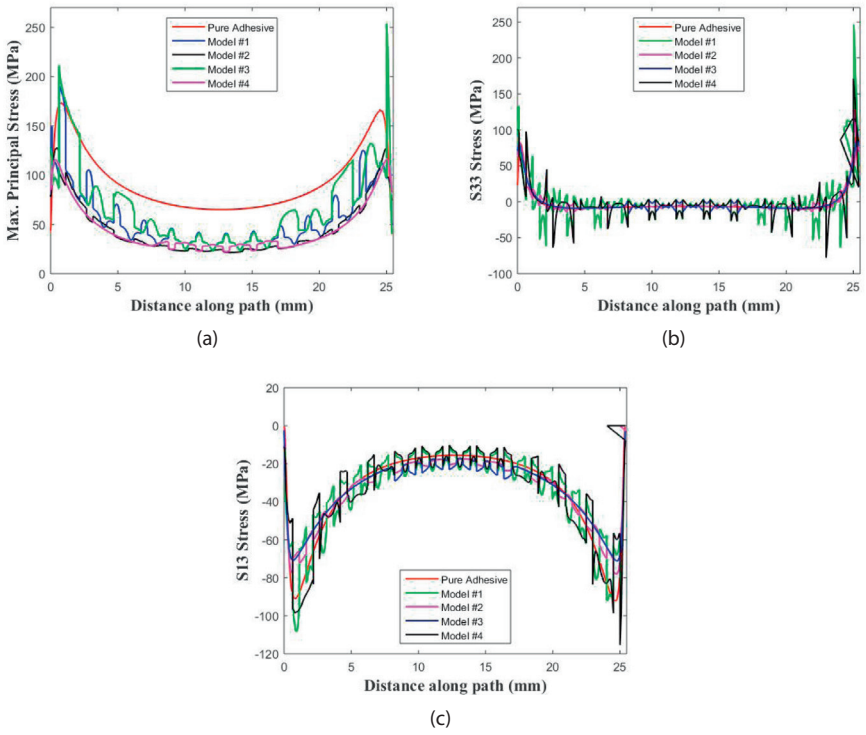

Fig. 8. (a) Maximum principal stress; (b) Normal stress in the thickness (33) direction; (c) Shear stress in 13 direction of pure epoxy and the 4 3D-PA models.

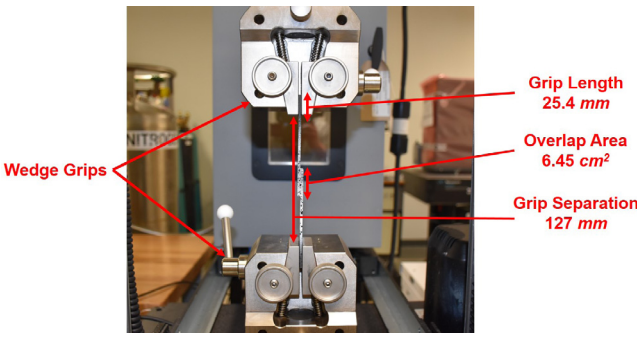

Fig. 9. Experimental setup of single lap shear tests.

SLS tests primarily involve tensile testing of single lap joint specimens that consist of two adherent substrates bonded together using an adhesive over an overlap area of 6.45 cm^2. The initial grip separation was 127 mm with 25.4 mm minimum grip length for samples at each end. Five samples for each bond type were prepared as mentioned before and tested at a loading rate of 13 mm/min. Fig. 9 shows the experimental set up for the lap shear test with corresponding dimensions.

5. Results and discussion

Failure modes in adhesively bonded joints have been widely studied by researchers, primarily focusing on the parameters leading to a certain failure mode. Predictive models of the same have

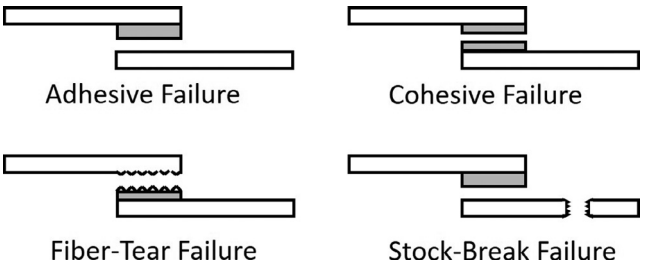

Fig. 10. Failure modes in lap shear tests.

been developed by earlier researchers [15,22–24] to capture the different failure mechanisms associated with adhesively bonded joints. Commonly observed failure modes related to lap shear tests are shown in Fig. 10.

SLS test data obtained from each test was post-processed to ultimately determine the apparent shear strength of the bonded joints. The load–displacement responses for each joint type are shown in Fig. 11 (a)–(f), which were analyzed to determine the peak load and energy absorbed by each sample. The limits of the axes are maintained constant between the figures to display the distinct differences in the response between different cases. It can be observed that 10:1 PA joints performed poorly as compared to that of 15:1 PA and Model 4 joints, where the latter manifested the highest strength and energy among all joint types. Also, an increase of 107.6%, 155.5%, 132.1%, and 130% in stiffness was observed in Models 1–4 as compared to that of 10:1 PA joints. However, when compared to 15:1 PA joints, Models 1–4 manifested a change of −3%, 19.3%, 8.5%, and 7.5%, respectively. The printed reinforcements appear to enhance the overall stiffness of the bonded joint. After assessing the load–displacement plots, the individual load values that were recorded by the operating load cell were divided by the overlapping bond area to calculate the apparent shear strengths of the joints. The average and standard deviation of shear strength values corresponding to adhesive and cohesive failure modes were independently determined following ASTM standards for each bond type, and are summarized in Fig. 12 (a). The corresponding energy absorption values were also calculated by determining the area under the load–displacement responses, and are summarized in Fig. 12 (b). A trend similar to that of shear strengths among different configurations is observed in the case of energy absorption as well.

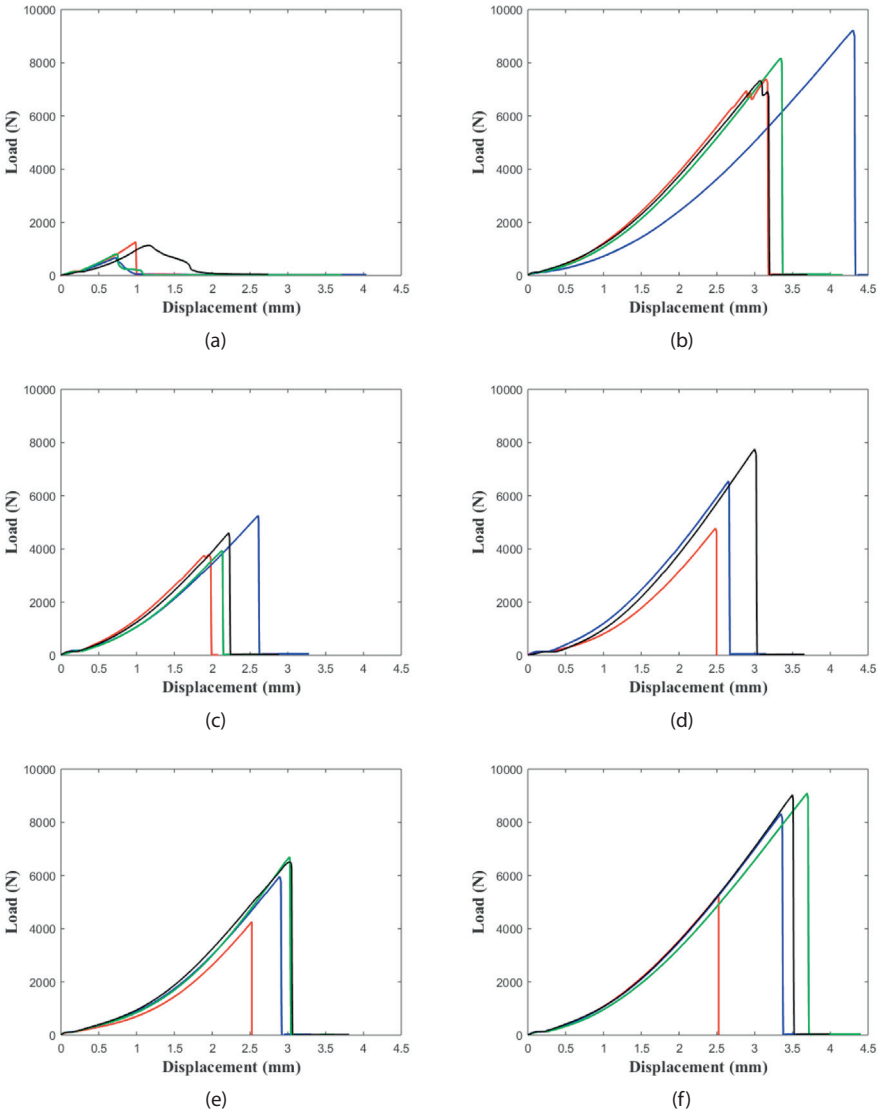

Fig. 11. Load vs. displacement responses for (a) PA (10:1), (b) PA (15:1), (c) Model 1, (d) Model 2, (e) Model 3, and (f) Model 4.

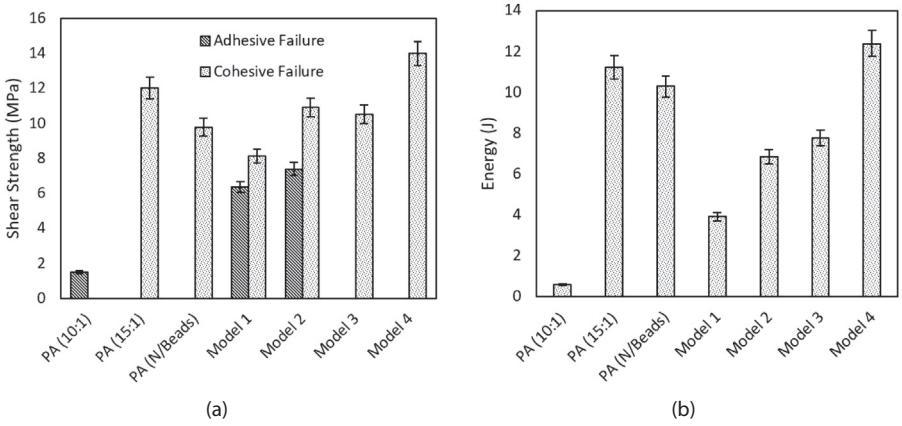

Fig. 12. (a) Summary of (a) shear strength values and (b) energy absorbed for all joint types investigated.

Adhesive and cohesive failures were the two key failure modes observed from the five joint types investigated. Adhesive failure was dominant in the case of 10:1 PA joints as shown in Fig. 13 (a), where the bond region separates from the adherent completely. Here, 10:1 PA joints represents the case where a mass ratio of 10:1 between the adhesive and microspheres as suggested by the manufacturer was used. The glass microspheres added to ensure a fixed bond thickness are visible in this figure. Cohesive failure was observed in one case only as shown in Fig. 13(c), where the failure region passed through the bond material. Cohesive failure was ignored due to its rare occurrence within the PA bonded joints tested. However, upon increasing the ratio of adhesive and microspheres to 15:1, the peak stress increased drastically and the failure mode was predominantly cohesive in nature. PA joints manufactured without microspheres showed an increase in shear strength with respect to 10:1 PA joints, while performing lower than 15:1 PA joints. Since the focus of this paper is not to investigate the influence of microsphere ratios on the bond strength, the comparisons henceforth are made with the results from the ratio specified by the manufacturer.

Models 1 and 2 3D-PA bonded joints displayed both adhesive and cohesive failures at the bond region as shown in Fig. 14, with the 3D designs visible in both types of failure. The corresponding peak loads and stresses increased by 323.4% for Model 1 and 393.1% for Model 2 as compared to the PA joints. Unlike Models 1 and 2, Models 3 and 4 3D-PA bonded joints displayed only cohesive failures at the bond region as shown in Fig. 15. Corresponding peak stresses showed an increase of 600.5% for Model 3 and 832.6% for Model 4 as compared to the PA joints, manifesting higher strengths than Models 1 and 2. This drastic increase in strength is attributed to the shift in failure mode from adhesive to cohesive failure, as well as resistance to shear failure caused by the 3D printed reinforcements. This initial study has shown that the structure imparted to the bond regions using 3D printing has significantly improved the shear strength of the bonded joints.

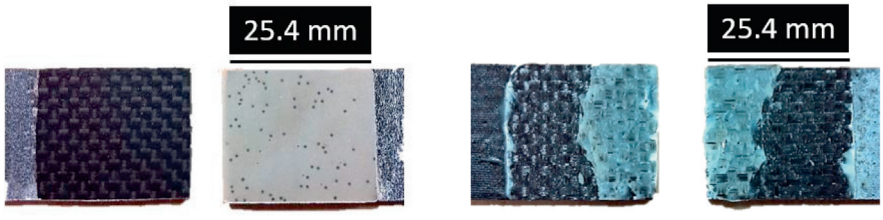

Fig. 13. Pure adhesive joints: (a) Top view of adhesive failure; (b) Top view of cohesive failure.

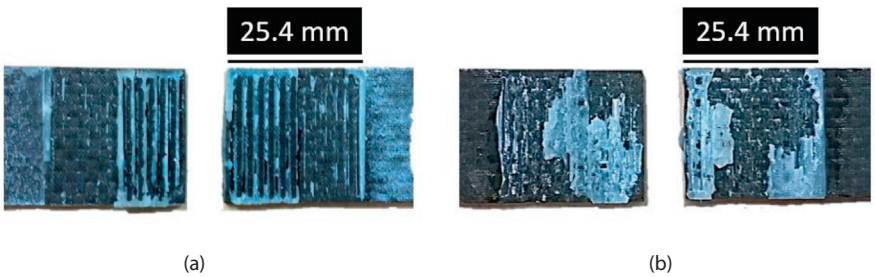

Fig. 14. (a) Top view of cohesive failure of 3D-PA Model 1; (b) Top view of cohesive failure of 3D-PA Model 2.

Fig. 15. (a) Top view of cohesive failure of 3D-PA Model 3; (b) Top view of cohesive failure of 3D-PA Model 4.

6. Summary/conclusion

Improvement in strength and toughness of adhesively bonded joints was achieved by fusing structural reinforcements to carbon woven laminate adherents using fused deposition modeling (FDM) additive technique. Single lap joints were fabricated with texture at the bond region imparted using polymer additive manufacturing technology. Pure adhesive (PA) joints were manufactured first, followed by the fabrication of 3D-printed adhesive (3D-PA) joints. Peak loads, shear stresses, and failure types were compared between each model. Computational analyses of PA and 4 designs of 3D-PA bonded joints were conducted prior to fabricating them. Stress concentrations along the bond line for each joint was determined and compared to explore the influence of bond patterns on the stress distribution.

Key observations from the research presented in this paper are as follows:

1. PA joints with epoxy/microsphere ratio of 10:1 failed mainly adhesively with a low average apparent shear strength value of 1.5 MPa. Whereas, PA joints with epoxy/microsphere ratio of 15:1 failed mainly cohesively with an average apparent shear strength value of 12.03 MPa.
2. 3D-PA joints manifested higher average peak loads and shear strength values as compared to PA joints with epoxy/microsphere ratio of 10:1. In particular, Model 4, with print lines only in the interior of the bond region, showed a maximum increase of up to ≈832% with respect to PA joints with 10:1 ratio and about ≈43% with respect to PA joints with no microspheres added to the epoxy.
3. A trend similar to that of shear strength was observed in the case of total energy absorbed between the different joint types, along with an increase in joint stiffness.
4. Printed reinforcements appear to have imparted higher shear resistance to the bond regions. Specifically, the stress distribution in the bond region is affected by the pattern imparted, which causes an improvement in the apparent shear strength of the single lap joints.

To summarize, a combined computational and experimental approach was used to established that the 3D printed reinforcements have the potential to drastically improve the apparent shear strength of adhesively bonded single lap joints.

Acknowledgements

The authors would like to acknowledge the support through the AFOSR Young Investigator Program award (Award No.: FA9550-15-1-0216) to conduct the research presented in this paper. In addition, the authors would like to thank Edgar Acuna for assisting with initial development of computational modeling presented in this work.

References

[1] Matthews FL, Kilty PPF, Godwin E. A review of the strength of joints in fiber-reinforced plastics 2: adhesively bonded joints. Composites 1982;13(1):29–37.
[2] Baldan A. Adhesively-bonded joints and repairs in metallic alloys, polymers and composite materials: adhesives, adhesion theories and surface pretreatment. J Mater Sci 2004;39(1):1–49.
[3] Davis MJ, Bond D. Principles and practise of adhesive bonded structural joints and repairs. Int J Adhesion Adhes 1999;19(3):91–105.
[4] Adams RD, Comyn J, Wake WC. Structural adhesive joints in engineering. Springer; 1997.
[5] Chamis CC, Murthy PLN. Simplified procedures for designing adhesively bonded composite joints. J Reinf Plast Compos 1991;10(1):29–41.
[6] Banea MD, da Silva LFM. Adhesively bonded joints in composite materials: An overview. Proc Inst Mech Eng, Part L: J Mater Des Appl 2009;223(1):1–18.
[7] Budynas RG, Nisbett JK, Shigley JE. Shigley's mechanical engineering design. McGraw-Hill; 2008. McGraw-Hill series in mechanical engineering.
[8] Osnes H, Andersen A. Computational analysis of geometric nonlinear effects in adhesively bonded single lap composite joints. Compos Part B: Eng 2003;34(5):417–27.
[9] Tong L. Bond strength for adhesive-bonded single-lap joints. Acta Mech 1996;117(1):101–13.
[10] Kim J-S, Kim CG, Hong CS. Practical design of tapered composite structures using the manufacturing cost concept. Compos Struct 2001;51(3):285–99.
[11] Kaye RH, Heller M. Through-thickness shape optimisation of bonded repairs and lap-joints. Int J Adhesion Adhes 2002;22(1):7–21.
[12] da Silva LFM, Adams R. Techniques to reduce the peel stresses in adhesive joints with composites. Int J Adhesion Adhes 2007;27(3):227–35.
[13] ASTM(D5868-014). Standard test method for lap shear adhesion for fiber reinforced plastic (frp) bonding. 2014.
[14] Boutar Y, Nami S, Mezlini S, Sik Ali MB. Effect of surface treatment on the shear strength of aluminium adhesive single-lap joints for automotive applications. Int J Adhesion Adhes 2016;67:38–43. Special Issue on Adhesion, Surface Preparation and Adhesive Properties.
[15] Kim KS, Yoo JS, Yi YM, Kim CG. Failure mode and strength of uni-directional composite single lap bonded joints with different bonding methods. Compos Struct 2006;72(4):477–85.
[16] Stapleton SE, Waas AM, Arnold SM. Functionally graded adhesives for composite joints. Int J Adhesion Adhes 2012;35:36–49.
[17] Justusson BP. The response of textile composites subjected to elevated loading rates. University of Michigan; 2015 [PhD Thesis].
[18] Henkel. Loctite ea e-120hp technical data sheet. p. 1; 2006.
[19] Stratasys Inc., Abs-m30 production-grade thermoplastic for fortus 3d production systems. p. 1; 2013.
[20] Lang TP, Mallick PK. The effect of recessing on the stresses in adhesively bonded single-lap joints. Int. J. Adhesion Adhes. 1999;19(4):257–71.
[21] Mazumdar SK, Mallick PK. Static and fatigue behavior of adhesive joints in smc-smc composites. Polymer Composites 1998;19(2):139–46.
[22] Kairouz KC, Matthews FL. Strength and failure modes of bonded single lap joints between cross-ply adherends. Composites 1993;24(6):475–84.
[23] Cheuk PT, Tong L. Failure of adhesive bonded composite lap shear joints with embedded precrack. Compos Sci Technol 2002;62(7–8):1079–95.
[24] Kumar SB, Sivashanker S, Bag A, Sridhar I. Failure of aerospace composite scarf-joints subjected to uniaxial compression. Mater Sci Eng: A 2005;412(1–2):117–22.